

Calibration of 3-D transient groundwater flow models for fractured rock

J. J. GÓMEZ-HERNÁNDEZ,

H. J. W. M. HENDRICKS FRANSSEN, A. SAHUQUILLO

Departamento de Ingeniería Hidráulica y Medio Ambiente, Universidad Politécnica de Valencia, C. Camino de Vera s/n, E-46011 Valencia, Spain

e-mail: harric@dihma.upv.es

J. E. CAPILLA

Departamento de Física Aplicada, Universidad Politécnica de Valencia, C. Camino de Vera s/n, E-46011 Valencia, Spain

Abstract The sequential self-calibrated method for the inverse modelling of groundwater flow has been extended to three-dimensional (3-D) transient groundwater flow and applied to fractured sites. Fractured sites are modelled using a stochastic continuum approach in which fractures induce higher conductivities in sets of blocks aligned according to predefined plane orientations. Two examples are presented demonstrating two different ways to incorporate fractures in the modelling process. In the first, fracture geometry is treated stochastically, with fractures distributed according to preferential planes. In the second, fracture geometry is treated deterministically. In both cases fractures are heterogeneous in their plane. The rest of the blocks represent an equivalent continuum that includes background fracturing and the rock matrix. The sequential nature of the self-calibration process highlights how conditioning to the different types of data (mainly conductivities and piezometric heads) imposes certain patterns of spatial variability in the final model.

INTRODUCTION

The sequential self-calibrated method for the stochastic inverse modelling of groundwater flow (Sahuquillo *et al.*, 1992; Gómez-Hernández *et al.*, 1997; Capilla *et al.*, 1997), was originally formulated for two-dimensional (2-D) steady state groundwater flow and has recently been extended to transient flow (Hendricks Franssen *et al.*, 1999a) and three-dimensional (3-D) flow in fractured media (Hendricks Franssen *et al.*, 1999b). Fractures are potential fast travel paths for contaminants; their characterization is therefore crucial for reliable contaminant travel time predictions. In this paper two different approaches are presented to handle fractures in the calibration of stochastic 3-D groundwater flow models. One approach incorporates the fractures stochastically; fracture geometry changes from one realization to another respecting the fracture positions' data available at the boreholes. The other approach incorporates the fractures deterministically; detailed geological investigations allow definition of the geometry of the fracture planes. In both cases, fractures are heterogeneous in their planes and their hydraulic conductivities are calibrated (to match measured piezometric heads) for a number of realizations.

THE SEQUENTIAL SELF-CALIBRATED METHOD

Below we summarize the steps in the sequential self-calibrated method (SCM). Details on the method can be found in Sahuquillo *et al.* (1992), Gómez-Hernández *et al.* (1997) and Capilla *et al.* (1997). In the description below we only refer to the calibration of hydraulic conductivity, however, other parameters like storativity (Hendricks Franssen *et al.*, 1999a) or boundary conditions may be subject to calibration, too. The steps are:

1. A seed 3-D $\log_{10} K$ realization is generated by standard geostatistical techniques. The realization is made conditional to hard and soft $\log_{10} K$ measurements.
2. The 3-D steady and/or transient groundwater flow equation is solved in this K field subject to given boundary (and initial) conditions. (Values for storativity, recharge and discharge must also be provided; these parameters may also be subject to calibration.)
3. The objective function defined as the weighted sum of squared differences between simulated and measured hydraulic head values at the locations and times that measurements are available, is evaluated. If the objective function value is below a user-predefined tolerance value, the $\log_{10} K$ realization is considered to be conditional to the hydraulic head data. The tolerance value is set considering the magnitude of the hydraulic head measurement errors.
4. If the objective function value is above the tolerance value, an iterative nonlinear optimization procedure is started. A $\log_{10} K$ perturbation field is calculated by minimizing the objective function, so that the solution of the flow equation in the field resulting as the sum of the realization in step 3 and this perturbation, matches the measured heads. For the minimization procedure and in order to reduce the dimensionality of the optimization problem, the $\log_{10} K$ perturbation field is parameterized as a function of the perturbation at a limited number of grid cells called master blocks. The perturbations at locations other than the master block locations are obtained by interpolation of the latter, i.e. by ordinary kriging.
5. Given the nonlinear dependence of the objective function on the parameter values, it is necessary in general to repeat steps 2 to 4 alternating different optimization algorithms until the objective function has reached a value below the tolerance.
6. Steps 1 to 5 are repeated for as many realizations as desired.

INCORPORATING FRACTURES

Two case studies are presented below in which the fractures are incorporated in the self-calibration approach in a different way. In the first case study, the main fractures in the site were classified into two main families with given orientations. Some fracture data had been collected in the boreholes but it was difficult to correlate most of these data across boreholes. As a result, fractures were treated as stochastic objects that are oriented parallel to two main planes and which honour the fracture intersections at the boreholes. In the second case study, the simulation domain is smaller, and the amount of data collected from boreholes larger, allowing the construction of a deterministic fracture model in which each fracture has known orientation and extent.

From the point of view of implementing the self-calibrated algorithm, the two methods differ in the way the perturbation field in step 4 above is computed. In the stochastic fracture approach, a perturbation is computed independently for each fracture family, whereas in the deterministic fracture approach, a perturbation is computed for each individual fracture. During the calculation of the perturbation, fracture geometry remains unchanged. (Note that an interesting extension of the self-calibrated approach would be the calibration/perturbation of the fracture geometry on the seed fields along with the material properties.)

STOCHASTIC FRACTURE GENERATION

The study (for reasons of confidentiality we cannot be more specific about the sites) in which fracture geometry is stochastic is presented first. The purpose was to study the uncertainty on groundwater flow and mass transport in a 3-D block of fractured volcanic tuff. The rock matrix has extremely low conductivity and the estimated equivalent conductivity of a block composed of rock matrix and joints is still very small. The site contains a large number of more conductive fractures that were thought to be the main paths for flow and transport. Geological investigations indicate that the main fractures can be classified into two families of sub-parallel fractures. The first and most abundant one has an azimuth northwest–southeast and dips 40° , the second one has an azimuth east-northeast–west-southwest and dips 70° . The conductivity fields are generated by considering three different populations: one for the non-fractured material and one for each of the two fracture families.

Generating the conductivity fields with fractures

The area under study is discretized into 50 by 50 blocks in the horizontal plane and 30 blocks in the vertical plane. All 75 000 blocks are cubic of size $20 \times 20 \times 20$ m. An interpretative structural model provided a tessellation of the main fractures in the study area. Given its interpretative nature, this structural model is used as soft information to condition the position of the blocks intersected by fractures. Some conductivity measurements are also available: 34 measurements were made in non-fractured blocks, 45 measurements in fracture family 1, and 5 measurements in fracture family 2. The histogram of the conductivity data is given in Fig. 1.

In order to simulate the hydraulic conductivity realizations variograms have to be provided. However, given the few hydraulic conductivity measurements available it was impossible to make any estimation, therefore, variograms were adopted: an isotropic spherical variogram with a range of 200 m for the non-fractured blocks, and two very anisotropic spherical variograms for each of the fracture families with the main directions of anisotropy on the planes of orientation of each fracture family. Geological information together with expert knowledge from studies carried out at other sites was used to decide on these variogram models.

Each of the two fracture families was generated independently of each other by sequential indicator simulation (Gómez-Hernández & Srivastava, 1990). For the indicator simulation, the structural geology model was used as soft conditioning data

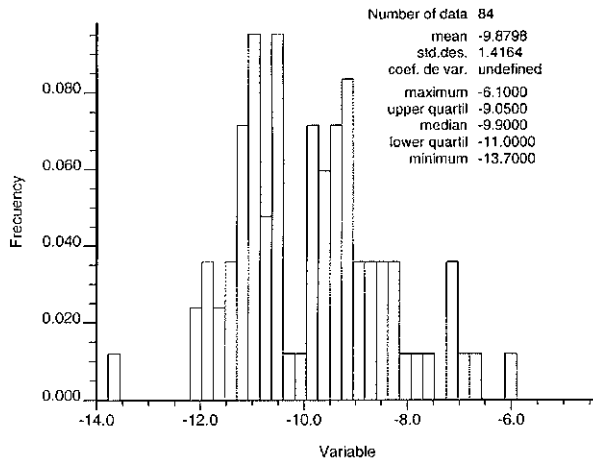


Fig. 1 Histogram of \log_{10} conductivity data.

by transforming them into prior probabilities of fracture presence. Once the fracture/non-fracture geometry model is built, each of the three populations (two fracture families and background) is completed with conductivity values generated by three independent sequential Gaussian simulations (Gómez-Hernández & Journel, 1993). Fracture geometry and material properties vary between realizations except at conditioning locations. Figure 2 shows one of the conductivity realizations. At this stage, the seed realization has been generated; this realization is not conditional to head data as yet.

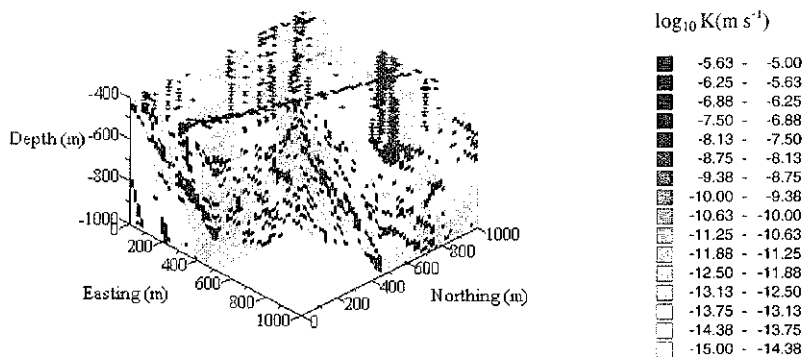


Fig. 2 3-D hydraulic conductivity image conditioned to both \log_{10} conductivity data and soft information from the structural model.

Conditioning of hydraulic head data

The next step in the self-calibrated algorithm is conditioning the seed field to the hydraulic conductivity measurements. Piezometric heads were monitored at 31 measurement locations during a constant head 158 m drawdown pumping test carried out in a packed-off section in the centre of the simulation domain. Given that the drawdowns did not propagate to the limits of the study area, it was enough to use

uniform zero heads at the boundaries as boundary conditions. As already mentioned, each one of the three facies considered (blocks intersected by any of the two fracture families and blocks representing the rock matrix plus background fracturing) was generated independently and then perturbed independently of each other. This means that the perturbation at any master block propagates within the nearby blocks in the same facies. However, from the point of view of fluid flow, all blocks interact together.

Results

A total of 50 simulations were generated using hydraulic conductivity measurements, structural geology, and hydraulic head drawdown data. The computational costs of the process of conditioning to the head drawdowns prevented the generation of a larger number of realizations. For a Monte-Carlo analysis of uncertainty in flow and transport predictions, a larger number of realizations would have been desirable. The reproduction of the measured drawdowns at the 31 monitoring locations is good, with the exception of a couple of locations for which it was impossible to improve the reproduction beyond a fair match. (This difficulty in reproducing the head data is uncommon in 2-D applications; in this particular case, the site is 3-D and the conductivity is very complex.)

Figure 3 shows the ensemble statistics of head values obtained after solution of the flow equation in the seed fields (before conditioning to hydraulic head drawdown) and in the final updated fields (after conditioning to hydraulic head drawdown data). Figure 3 shows an initially highly anisotropic head drawdown response produced by the presence of fractures and the large contrast imposed between fractured and unfractured blocks. However, after conditioning to the experimental head drawdown data, the simulated head drawdowns are much more isotropic, indicating that the large contrast introduced in the seed fields was too large, and that contrary to initial belief in the

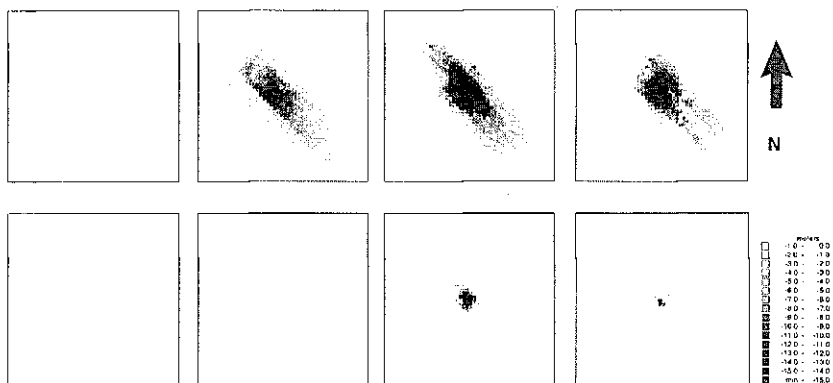


Fig. 3 Ensemble average head drawdown at four horizontal slices as simulated in the seed fields (top row) and in the updated fields (bottom row). The slices are at 400, 500, 600 and 700 m below OD. The constant head drawdown was imposed at 660 m below OD. The head drawdowns for the horizontal slices in the top row are 0.0, 16.09, 46.75 and 23.33 m respectively. The head drawdowns for the horizontal slices in the bottom row are 0.0, 2.95, 29.96 and 9.04 m going from left to right. White = 0 to -1 m, black = -15m to min.

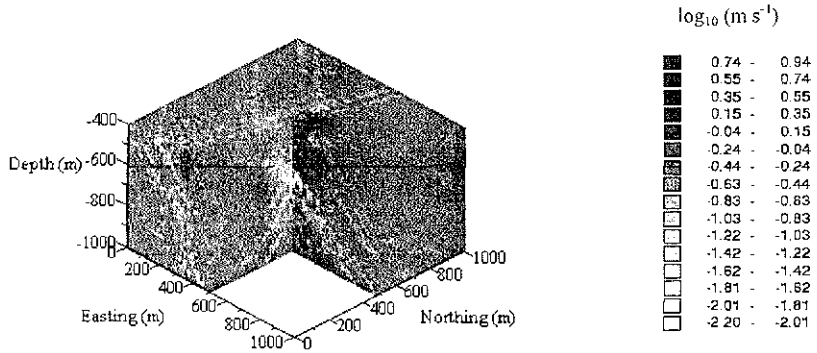


Fig. 4 Average perturbation applied to the seed log conductivity fields in order to achieve conditioning to the hydraulic head drawdowns. Light shades correspond to a reduction in conductivity (as low as two orders of magnitude), dark shades correspond to an increase in conductivity (as large as one order of magnitude).

flow response of the block, the background fracturing has an important effect. Figure 4 shows the average perturbation applied to the seed hydraulic conductivity fields in order to condition them to the measured head drawdown data. The hydraulic conductivity of the non-fractured blocks has increased by about one order of magnitude around the pumping location, while the hydraulic conductivity of many of the fractures decreases by about two orders of magnitude.

DETERMINISTIC FRACTURE GENERATION

In the deterministic fracture generation, the geometry of each fracture is known and, in this particular case, given by the equation of a plane. These equations have been obtained from detailed geological observations. As in the previous case study, blocks were classified as fractured if they are intersected by any fracture, or unfractured, in which case they represent the equivalent conductivity of the rock matrix and the background joints. A total of 20 fracture planes were defined. These fracture planes remain fixed for all realizations. Sequential simulation is used to generate the seed hydraulic conductivities for each fracture. Each generation is made independently for each fracture and conditioned to the hydraulic conductivity measurements available in that fracture plane.

Generating the conductivity field with fractures

The purpose of the second study is to characterize a fractured block of granite in order to make groundwater flow and mass transport predictions. The area modelled extends 247 m × 227 m × 287 m, and is discretized into 37 × 34 × 43 cubic cells of 6.67 m size. The available data consists of 122 conductivity data derived from packer tests conducted in four boreholes drilled through the study area. Of the 122 data, 101 characterize unfractured blocks and 21 characterize fractured blocks. In addition, detailed geological investigations have defined 20 fractures which are modelled as

planar with given orientations and extent. All 20 fractures serve to classify, in a deterministic manner, all blocks in the numerical model as either fractured or unfractured. Figure 5 shows a 3-D view of this classification.

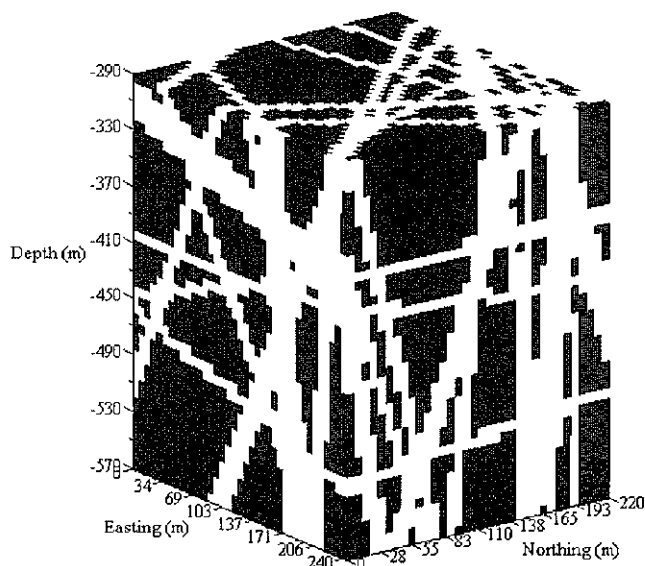


Fig. 5 Structural model of the area under study. White corresponds to fracture and dark to unfractured material.

Hydraulic conductivities are assigned independently to each of the 20 different fracture planes and the unfractured blocks. Sequential Gaussian simulation is the method used for the simulation. The log conductivities are drawn from the same multi-lognormal distribution for each of the fractures, namely, with a mean of $-6.5 \log_{10} \text{ m s}^{-1}$, a variance of 1 and an isotropic (in the fracture plane) spherical variogram with a range of 40 m. Similarly, the log conductivities of the unfractured blocks are drawn from a multiGaussian distribution with a mean of $-10.0 \log_{10} \text{ m s}^{-1}$, a variance of 1 and isotropic spherical variogram of 40 m. In all cases, the distributions are conditioned to the measured values in the given fracture. The mean and variance of the multiGaussian distributions used are derived from the sample data; the variogram has to be imposed given the lack of data to compute reliable variogram estimates. It should be noted that it is assumed, in the generation of the seed fields, that all fractures have the same degree and type of heterogeneity. Figure 6 shows a hydraulic conductivity seed realization.

Incorporating hydraulic information

The hydraulic conductivity seed field is then conditioned to steady state hydraulic head measurements and to the measured drawdowns resulting from 24 interference tests. Of the 24 pumping tests available, only seven were used to condition the final fields due

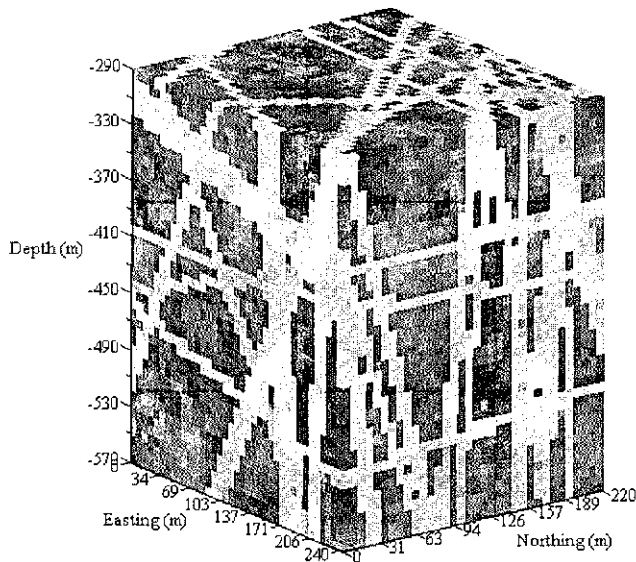


Fig. 6 3-D hydraulic conductivity seed realization. It is only conditioned to \log_{10} conductivity data and the structural information. Values of $\log_{10} K$ range from -3 to -13 , the light shades corresponding to the higher conductivity values.

to computer resource limitations. Let us recall that conditioning to head measurements means that the numerical solution of the flow equation in the conditioned hydraulic conductivity fields matches the head values at their measurement locations.

Of the seven pumping test to which the final updated conductivity realization is conditioned, five are short-term (30 min) and have a local effect around the pumping location, and one is long-term (16 days) with a larger effect within the study area. One of the interesting results is to monitor the evolution of the average hydraulic conductivities in each of the fractures as the conditioning progresses. Table 1 gives these mean values for the seed log conductivity fields (conditioned only to log conductivity data), for the log conductivity fields after additional conditioning to steady state head data, and for the log conductivity fields after conditioning to both steady state and transient head data. The difference between the means in the seed fields and the means in the fields conditioned to all head data is also reported. It can be seen that, on average, the log conductivity of the unfractured blocks does not vary. However, there are fractures for which this change is noticeable. For instance, fracture number 5 increases its average value by almost two orders of magnitude, while fracture number 6 decreases it by 1.5 orders of magnitude. These changes allow differentiation of the importance of each fracture in the flow behaviour of the area under study, differentiation which is impossible to perform on the basis of the small number of local conductivity measurements and that can only qualitatively be guessed after the analysis of the interference tests. The histograms of log conductivity in the fractures (not shown) evolve from close to Gaussian to negatively skewed, with the net effect of an increase of within fracture heterogeneity. Another, interesting conclusion which can be drawn from Table 1 is that the most informative head information, in this case study,

Table 1 Evolution of fracture average conductivities as piezometric head information is used in the conditioning process.

	Conditioned to K (1)	Conditioned to K and steady h (2)	Conditioned to K , steady h and transient h (3)	Total perturbation (3) - (1)
Non-fractured	-10.12	-9.83	-10.19	-0.07
Fracture 1	-6.47	-6.54	-6.54	-0.07
Fracture 2	-6.32	-6.22	-6.34	-0.02
Fracture 3	-6.47	-6.40	-6.46	+0.01
Fracture 4	-6.44	-7.30	-7.32	-0.88
Fracture 5	-6.55	-4.98	-4.62	+1.93
Fracture 6	-6.75	-8.18	-8.29	-1.54
Fracture 7	-6.39	-7.27	-7.37	-0.98
Fracture 8	-6.41	-4.78	-5.38	+1.03
Fracture 9	-6.56	-8.05	-8.02	-1.46
Fracture 10	-6.29	-7.57	-7.41	-1.12
Fracture 11	-6.55	-7.93	-7.77	-1.22
Fracture 12	-6.48	-6.55	-6.59	-0.11
Fracture 13	-6.51	-7.75	-7.59	-1.08
Fracture 14	-6.27	-5.42	-5.32	+0.95
Fracture 15	-6.28	-6.19	-5.90	+0.38
Fracture 16	-6.22	-6.77	-7.04	-0.82
Fracture 17	-6.40	-5.98	-5.52	+0.88
Fracture 18	-6.44	-6.35	-6.58	-0.14
Fracture 19	-6.30	-7.20	-7.13	-0.83
Fracture 20	-6.30	-6.33	-6.32	-0.02

are the steady state values. The largest update occurs after calibration to steady-state data, with a smaller modification after conditioning to transient values. Probably this latter effect is due to the local impact of the pumping tests used for conditioning.

CONCLUSIONS

Two studies were presented demonstrating the application of the self-calibrated method to 3-D fractured media. The two studies differ in the way the fractures are treated in the model. In the first study, the position of the fractures is stochastic and soft conditioned by a structural model. Then, for the head conditioning, only three populations are considered. In the second study, the fractures are incorporated deterministically. However, for the head conditioning, a different population is considered for each of the fractures.

Whether to use stochastic or deterministic fracture geometry depends on the amount and precision of the information available. An important extension of the self-calibrated method would be to also include the fracture geometry in the conditioning process.

The conductivity realizations were conditioned successfully to the steady state and transient state hydraulic head measurements, in a 3-D numerical model with several

tens of thousands of blocks. In both studies, the value of the head data demonstrated by the evolution of the conductivity fields before and after conditioning to head measurements, was shown. In the first study, the contrast between fractured and unfractured blocks is substantially reduced. The second study shows how the conductivities of individual fractures evolve with conditioning.

REFERENCES

- Capilla, J. E., Gómez-Hernández, J. J. & Sahuquillo, A. (1997) Stochastic simulation of transmissivity fields conditional to both transmissivity and piezometric data. 2. Demonstration on a synthetic aquifer. *J. Hydrol.* **203**(1–4), 175–188.
- Gómez-Hernández, J. J. & Journel, A. G. (1993) Joint simulation of multiGaussian random variables. In: *Geostatistics Tróia '92*, vol. 1 (ed. by A. Soares), 85–94. Kluwer, Dordrecht, The Netherlands.
- Gómez-Hernández, J. J., Sahuquillo, A. & Capilla, J. E. (1997) Stochastic simulation of transmissivity fields conditional to both transmissivity and piezometric data. 1. Theory. *J. Hydrol.* **203**(1–4), 162–174.
- Gómez-Hernández, J. J. & Srivastava, R. M. (1990) ISIM3D: an ANSI-C three dimensional multiple indicator conditional simulation program. *Computer and Geosciences* **16**(4), 395–400.
- Hendricks Franssen, H. J. W. M., Gómez-Hernández, J. J., Capilla, J. E. & Sahuquillo, A. (1999a) Joint simulation of transmissivity and storativity fields conditional to hydraulic head data. *Adv. Wat. Resour. Res.* **23**, 1–13.
- Hendricks Franssen, H. J. W. M., Cassiraga, E. F., Gómez-Hernández, J. J., Sahuquillo, A. & Capilla, J. E. (1999b) Inverse modeling of groundwater flow in a 3D fractured medium. In: *GeoENV II—Geostatistics for Environmental Applications* (ed. by J. J. Gómez-Hernández, A. Soares & R. Froidevaux), 283–294. Kluwer, Dordrecht, The Netherlands.
- Sahuquillo, A., Capilla, J. E., Gómez-Hernández, J. J. & Andreu, J. (1992) Conditional simulation of transmissivity fields honoring piezometric data. In: *Hydraulic Engineering Software IV, Fluid Flow Modeling* (ed. by W. R. Blain & E. Cabrera), 201–214. Elsevier Applied Science, London, UK.